Administration of chitosan-tripolyphosphate-DNA nanoparticles to knockdown glutamate dehydrogenase expression impairs transdeamination and gluconeogenesis in the liver

Carlos Gaspar[a], Jonás I. Silva-Marrero[a], Anna Fàbregas[b], Montserrat Miñarro[b], Josep R. Ticó[b], Isabel V. Baanante[a] and Isidoro Metón[a,*]

[a]Secció de Bioquímica i Biologia Molecular, Departament de Bioquímica i Fisiologia, Facultat de Farmàcia i Ciències de l'Alimentació, Universitat de Barcelona, Barcelona, Spain

[b]Departament de Farmàcia i Tecnologia Farmacèutica, i Fisicoquímica, Facultat de Farmàcia i Ciències de l'Alimentació, Universitat de Barcelona, Barcelona, Spain

***Correspondence:** Isidoro Metón, Secció de Bioquímica i Biologia Molecular, Departament de Bioquímica i Fisiologia, Facultat de Farmàcia i Ciències de l'Alimentació, Universitat de Barcelona, Joan XXIII 27-31, 08028 Barcelona, Spain. Tel.: +34 934024521; Fax: +34 934024520; **E-mail:** imeton@ub.edu

Abstract

Glutamate dehydrogenase (GDH) plays a major role in amino acid catabolism. To increase the current knowledge of GDH function, we analysed the effect of GDH silencing on liver intermediary metabolism from gilthead sea bream (*Sparus aurata*). Sequencing of GDH cDNA from *S. aurata* revealed high homology with its vertebrate orthologues and allowed us to design short hairpin RNAs (shRNAs) to knockdown GDH expression. Following validation of shRNA-dependent downregulation of *S. aurata* GDH *in vitro*, chitosan-tripolyphosphate (TPP) nanoparticles complexed with a plasmid encoding a selected shRNA (pCpG-sh2GDH) were produced to address the effect of GDH silencing on *S. aurata* liver metabolism. Seventy-two hours following intraperitoneal administration of chitosan-TPP-pCpG-sh2GDH, GDH mRNA levels and immunodetectable protein decreased in the liver, leading to reduced GDH activity in both oxidative and reductive reactions to about 53-55 % of control values. GDH silencing decreased glutamate, glutamine and aspartate aminotransferase activity, while increased 2-oxoglutarate content, 2-oxoglutarate dehydrogenase activity and 6-phosphofructo-1-kinase/fructose-1,6-bisphosphatase activity ratio. Our findings show for the first time that GDH silencing reduces transdeamination and gluconeogenesis in the liver, hindering the use of amino acids as gluconeogenic substrates and enabling protein sparing and metabolisation of dietary carbohydrates, which would reduce environmental impact and production costs of aquaculture.

Keywords: Glutamate dehydrogenase; Chitosan; Nanoparticles; Gene knockdown; Liver; *Sparus aurata*

1. Introduction

Glutamate dehydrogenase (GDH) plays a major role in amino acid catabolism and ammonia detoxification in the liver and kidneys through the catalysis of reversible oxidative deamination of L-glutamate to form α-ketoglutarate and ammonia using $NAD(P)^+$ as cofactor (Lushchak et al., 2008). GDH is a homohexameric enzyme located in the mitocondrial matrix that shows preferential

50 reactivity towards the intramitochondrial NADP(H) pool in both reaction directions *in vitro*, and a
51 near-equilibrium reaction with the NAD(H) pool. Flux direction of GDH catalysis remains a matter
52 of debate. Nevertheless, the high K_m value of ammonia and NAD^+/NADH ratio may direct catalysis
53 towards oxidative deamination (Karaca et al., 2011; Treberg et al., 2014). GDH activity is
54 allosterically regulated by a wide array of metabolites in a complex, still not well-understood
55 manner. GTP strongly inhibits GDH, while ADP activates the enzyme activity. GTP binding to
56 GDH is antagonised by phosphate and ADP, but is synergistic with NADH. Leucine and other
57 monocarboxylic acids also activate GDH, while palmitoyl-CoA, diethylstilbestrol and cystein-
58 specific ADP-ribosylation inhibit GDH activity (Li et al., 2014; Plaitakis et al., 2017). It was
59 suggested that glucose-dependent intracellular formation of glutamate by GDH might amplify
60 glucose-stimulated insulin secretion in pancreatic β-cells (Göhring and Mulder, 2012; Karaca et al.,
61 2011). Involvement of GDH in insulin secretion was emphasised by the fact that loss of allosteric
62 inhibition of GDH disturbs insulin secretion. In this regard, activating mutations of GDH cause the
63 hyperinsulinemia and hyperammonemia syndrome in humans. Indeed, overexpression of GDH in
64 mice increases insulin secretion (Carobbio et al., 2004), whereas GDH inhibition in pancreatic β-
65 cells impairs insulin secretion (Carobbio et al., 2009).

66 In fish, the molecular role of GDH remains largely unexplored. Glutamate is primarily
67 deaminated by GDH in the fish liver leading to concomitant production of ammonia, while in
68 mammals most glutamate is transaminated to aspartate (Peres and Oliva-Teles, 2006). The effect of
69 nutritional status on hepatic GDH depends on both species and diet composition. Fasting increases
70 GDH activity and/or mRNA levels in *Oncorhynchus mykiss*, *Protopterus dolloi*, *Dentex dentex* and
71 *Danio rerio* (Frick et al., 2008; Pérez-Jiménez et al., 2012; Sánchez-Muros et al., 1998; Tian et al.,
72 2015). However, starvation did not affect GDH activity in *Salmo gairdneri* (Tranulis et al., 1991)
73 and decreased GDH expression in *Dicentrarchus labrax* and *Sparus aurata* (Gaspar et al., 2018;
74 Pérez-Jiménez et al., 2007). High-protein diets stimulate growth and increase plasma free amino
75 acids, which in turn enhance GDH deamination and ammonia excretion (Bibiano Melo et al., 2006;
76 Borges et al., 2013; Caballero-Solares et al., 2015; Coutinho et al., 2016; Viegas et al., 2015). In *S.*
77 *aurata*, dietary supplementation with glutamate increases protein retention by stimulation of hepatic

78 glucose metabolism and down-regulation of GDH mRNA levels and reductive GDH activity
79 (Caballero-Solares et al., 2015), while dietary starch decreases GDH activity (Couto et al., 2008).
80 To better understand the functional role of GDH in the liver, we explored the metabolic effects
81 resulting from administration of chitosan-tripolyphosphate (TPP) nanoparticles complexed with a
82 short hairpin RNA (shRNA)-expression plasmid to knockdown GDH expression in the liver of *S.*
83 *aurata*.
84
85 **2. Materials and methods**
86 *2.1. Rearing procedures*
87 Gilthead seabream (*S. aurata*) juveniles obtained from Piscimar (Burriana, Castellón, Spain)
88 were maintained at 20 ºC in 260-L aquaria as described (Fernández et al., 2007). Fish were fed daily
89 40 g/kg body weight (BW) of a diet containing 58.0 % protein, 9.9 % lipids, 15.0 % carbohydrates,
90 15.4 % ash, 1.7 % moisture and 20.1 kJ/g gross energy. Chitosan-TPP nanoparticles were
91 intraperitoneally injected alone or complexed with 10 μg/g BW of pCpG-sh2GDH or pCpG-
92 siRNA-Scramble (control plasmid that expresses a scramble sequence with no homology with
93 known sequences; InvivoGen, San Diego, CA, USA). Seventy-two hours post-treatment, fish were
94 sacrificed by cervical section and the liver was immediately dissected out, frozen in liquid N_2 and
95 kept at -80 °C until use. To prevent stress, fish were anesthetised before handling with tricaine
96 methanesulfonate (1:12,500). Experimental procedures involving fish complied with the guidelines
97 of the University of Barcelona's Animal Welfare Committee and EU Directive 2010/63/EU for
98 animal experiments.
99
100 *2.2. Molecular cloning of GDH coding domain sequence from S. aurata*
101 The full-coding sequence of *S. aurata* GDH was isolated with the First Choice RLM-RACE
102 Kit (Thermo Fisher Scientific, Waltham, MA, USA) and primers designed from a partial *S. aurata*
103 GDH sequence (GenBank accession no. **JX073708**). Nested PCR was performed with gene-specific

104 primers CG1307 and CG1308 for 5'-RACE, as well as CG1306 and CG1305 for 3'-RACE (Table
105 1). RACE products were ligated into pGEM-T Easy (Promega, Madison, WI, USA) and sequenced
106 on both strands. The full-coding sequence of *S. aurata* GDH was amplified from the liver by RT-
107 PCR using primer pair CG1333/CG1334 (Table 1), ligated into pGEM-T Easy to generate pGEM-
108 GDH, and fully sequenced.
109
110 *2.3. Expression plasmids*
111 To generate pcDNA3-GDH, the coding domain sequence of GDH was amplified by PCR
112 using primer pair CG1526/CG1527 and pGEM-GDH as template. The resulting fragment was
113 digested with *Bam*HI and *Eco*RI and ligated into pcDNA3 (Life Technologies, Carlsbad, CA, USA)
114 previously digested with the same enzymes. To obtain pCpG-sh1GDH, pCpG-sh2GDH, pCpG-
115 sh3GDH, pCpG-sh4GDH and pCpG-sh5GDH, oligonucleotide pairs CG1531/CG1532,
116 CG1533/CG1534 CG1535/CG1536, CG1537/CG1538 and CG1539/CG1540 (Table 1),
117 respectively, were mixed at a final concentration of 25 μM each, heated a 90 ºC for 5 min and
118 cooled down at room temperature. One hundred ng of double-stranded products were ligated into
119 pCpG-siRNA (InvivoGen, San Diego, CA, USA) previously digested with *Hin*dIII and *Acc*65I.
120 shRNA sequences were designed using siRNA Wizard software (InvivoGen, San Diego, CA, USA).
121
122 *2.4. Preparation and characterisation of chitosan-TPP-DNA nanoparticles*
123 Chitosan-TPP nanoparticles complexed with pCpG-siRNA-Scramble or pCpG-sh2GDH were
124 prepared following the ionic gelation method as described (González et al., 2016). Three-hundred
125 μg of pCpG-siRNA-Scramble or pCpG-sh2GDH were added to 1.2 ml of 0.84 mg/ml TPP.
126 Thereafter, TPP-DNA solutions were added dropwise to 3 ml of 2 mg/ml low molecular weight
127 chitosan-acetate buffer (1:0.4 chitosan/TPP ratio). Chitosan-TPP-DNA nanoparticles were pelleted,
128 rinsed twice with ultrapure water and resuspended in 2 ml of 2 % w/v mannitol as cryoprotector

129 during lyophilisation. After a freeze–dry cycle at −47 °C, an additional drying step was performed
130 at 25 °C to remove residual water. Chitosan-TPP-DNA nanoparticles were characterised by atomic
131 force microscopy using peak force tapping mode (Multimode 8 AFM attached to a Nanoscope III
132 Electronics, Bruker, USA). *Z* potential was determined using laser Doppler microelectrophoresis in
133 a Zetasizer NanoZ equipped with DTS1060 capillary cells (Malvern Instruments, Malvern, UK).
134 Chitosan-TPP-DNA nanoparticles were resuspended in 0.9 % NaCl previous administration to *S.*
135 *aurata*.
136
137 *2.5. Cell culture and transfection*
138 HepG2 cells (ATCC HB 8065) were cultured in DMEM supplemented with 2 mM glutamine,
139 110 mg/l sodium pyruvate, 10 % foetal bovine serum, 100 IU/ml penicillin and 100 μg/ml
140 streptomycin. Cells were grown at 37 ºC and 5 % CO_2 in 6-well plates. The calcium phosphate
141 coprecipitation method (Graham and van der Eb, 1973) was used for transient transfection of
142 HepG2 cells at 45-50 % confluence with 30-300 ng pcDNA3-GDH, 600 ng of pCpG-siRNA-
143 Scramble or GDH-specific shRNA expression constructs, and 300 ng pCMV-β (*lac*Z) to correct for
144 variations in transfection efficiency. Empty plasmids were added to each transfection to ensure
145 equal DNA amounts. Forty-eight hours post-transfection, the cells were harvested, washed in PBS
146 and lysed to isolate total RNA. β-Galactosidase activity in 20-50 μl of the clear lysate was
147 measured as described (Metón et al., 2006).
148
149 *2.6. Quantitative RT-PCR*
150 One μg of total RNA isolated from HepG2 cells or *S. aurata* liver was reverse-transcribed to
151 cDNA using random hexamer primers and Moloney murine leukaemia virus RT (Life technologies,
152 Carsbad, CA, USA) for 1 h at 37 ºC. *S. aurata* GDH mRNA levels were determined in a Step One
153 Plus Real Time PCR System (Applied Biosystems, Foster City, CA, USA) in a 20-μl mixture

154 containing 0.4 μM of each primer, 10 μl of SYBR Green (Applied Biosystems, Foster City, CA,
155 USA), and 1.6 μl of diluted cDNA. The temperature cycle protocol for amplification was 95 °C for
156 10 min, followed by 40 cycles with 95 °C for 15 s and 62 °C for 1 min. A dissociation curve was
157 run after each experiment to confirm single product amplification. Amplification specificity was
158 confirmed by sequencing. *S. aurata* GDH mRNA was amplified with primer pair CG1543/CG1544
159 (Table 1). The expression of *S. aurata* GDH in transfected HepG2 cells was normalised with
160 ribosomal subunit 18s (primer pair MC109/MC110; Table 1) and β-galactosidase (primer pair
161 JDRTCMVBS/JDRTCMVBAS; Table 1). For *in vivo* experiments, mRNA levels were normalised
162 with *S. aurata* ribosomal subunit 18s, β-actin and elongation factor 1 α (EF1α) using primer pairs
163 JDRT18S/JDRT18AS, QBACTINF/QBACTINR and AS-EF1Fw/AS-EF1Rv, respectively (Table
164 1). Variations in gene expression were calculated by the standard $\Delta\Delta C_T$ method (Pfaffl, 2001).
165
166 *2.7. Western blotting analysis*
167 Liver extracts were loaded to a 10% SDS-PAGE gel. After electrophoresis, the gel was
168 equilibrated in transfer buffer (25 mM Tris-HCl, 192 mM glycine, 20 % methanol, pH 8.3) and
169 electroeluted onto a polyvinylidene fluoride membrane for 3 hours at 60 V and 4 ºC. After
170 incubation in blocking buffer (non-fat skim milk powder 5 % w/v, 50 mM Tris-base pH 7.5, 100
171 mM NaCl, 0.1 % Tween 20), the membrane was exposed to rabbit anti-GDH (OriGene, Rockville,
172 MD, USA) and mouse anti-actin (Sigma-Aldrich, Saint Louis, MO, USA) as primary antibodies
173 (1:1000). Immunodetection was performed using an alkaline phosphatase-conjugated secondary
174 antibody (Sigma-Aldrich, Saint Louis, MO, USA; 1:3000) and the Clarity Western ECL Substrate
175 Kit (Bio-Rad, Hercules, CA, USA).
176
177 *2.8. Enzyme activity assays and metabolite determinations*

178 Liver crude extracts for enzyme activity assays were obtained as described (Caballero-Solares
179 et al., 2015). GDH was assayed in the direction of L-glutamate formation (reductive reaction) by
180 monitoring NADH oxidation at 340 nm in a 250-μl mixture containing 50 mM imidazole-HCl pH
181 7.4, 250 mM ammonium acetate, 5 mM 2-oxoglutarate, 0.1 mM NADH, 1 mM ADP and 4 μl crude
182 extract. To measure GDH reaction in the direction of 2-oxoglutarate synthesis (oxidative reaction),
183 NADH formation was followed at 340 nm in a 200-μl assay containing 154 mM tris-HCl pH 9.0, 20
184 mM L-glutamate, 100 mM hydrazine, 1 mM NAD^+, 1 mM ADP and 4 μl crude extract. 2-
185 Oxoglutarate dehydrogenase (OGDH) activity was assayed after addition of 0.12 mM coenzyme A
186 to a final volume of 200 μl containing 50 mM phosphate buffer pH 7.4, 2 mM $MgCl_2$, 0.6 mM
187 thiamine pyrophosphate, 2 mM NAD^+, 10 mM 2-oxoglutarate, 0.2 mM EGTA, 0.4 mM ADP and 4
188 μl crude extract. Alanine aminotransferase (ALT) and aspartate aminotransferase (AST) were
189 determined with commercial kits (Linear Chemicals, Montgat, Barcelona, Spain). 6-Phosphofructo-
190 1-kinase (PFK), fructose-1,6-bisphosphatase (FBP1) and total protein were assayed as described
191 (Metón et al., 1999). One unit of enzyme activity was defined as the amount of enzyme necessary to
192 transform 1 μmol of substrate per min. 2-Oxoglutarate was determined by monitoring NADH
193 oxidation at 340 nm in a 200-μl assay containing 50 mM imidazole-HCl pH 7.4, 0.1 mM NADH,
194 0.37 U/mL GDH and 75 μl liver trichloroacetic acid extract. Spectrophotometric determinations
195 were performed at 30 °C in a Cobas Mira S analyser (Hoffman-La Roche, Basel, Switzerland).
196
197 *2.9. Amino acid analysis*
198 Amino acids and related molecules were analysed on filtered liver trifluoroacetic acid extracts
199 by cation-exchange chromatography followed by post-column derivatisation with ninhydrin and
200 UV/VIS detection (Moore et al., 1958). Chromatographic separation was performed using a
201 Biochrom 30 amino acid analyser equipped with PEEK column packed with Ultropac cation-

202 exchange resin (Lithium High Performance Physiological Column) and Peltier heating/cooling
203 system (Biochrom, Cambridge, UK). Following sample injection, a gradient elution was applied by
204 combining five lithium citrate buffers of increasing pH (2.80 to 3.55) and ionic strength (0.2 M to
205 1.65 M). Column effluents reacted with ninhydrin at 135 ºC and derivatised amino acids were
206 detected at 570 nm and 440 nm wavelenghts. Amino acid peaks were identified according to the
207 retention times of amino acid standards. Addition of L-norleucine to each sample allowed
208 calculation of amino acid concentration by the internal standard method. Data analysis was
209 performed with EZChrom Elite software (Agilent Technologies, Santa Clara, CA, USA).
210
211 *2.10. Statistics*
212 Analyses were performed with SPSS software Version 22 (IBM, Armonk, NY, USA).
213 Statistical analysis with two levels was determined using Student's *t* test. One-way ANOVA
214 statistical differences among three or more levels were determined with the Bonferroni post hoc
215 test.
216
217 **3. Results**
218 *3.1. Molecular cloning of the full-coding sequence of* S. aurata *GDH*
219 A 2,715 bp cDNA encoding GDH was isolated by RACE PCR performed on total RNA from
220 *S. aurata* liver. The *S. aurata* GDH nucleotide sequence was deposited to the GenBank database
221 under accession no. **MF459045**. The GDH cDNA contains a 1,629-bp open reading frame and a
222 consensus polyadenylation signal (AATAAA) 20 bp upstream from the poly(A+) tail. The deduced
223 amino acid sequence of *S. aurata* GDH predicts a polypeptide of 542 residues with a calculated
224 molecular mass of 59.67 kDa. Computer analysis with TargetP 1.1 (Emanuelsson et al., 2000;
225 Nielsen et al., 1997) indicated that GDH cDNA contains a mitochondrial targeting peptide with
226 putative cleavage site at position 20. The inferred amino acid sequence of *S. aurata* GDH was

227 aligned with GDH orthologues in other vertebrates to explore evolutionary relationships (Fig. 1A).
228 *S. aurata* GDH retains all residues considered important for glutamate and GTP binding (15 and 16
229 residues, respectively) and most residues involved in the binding to NAD^+ (20 out of 25), ADP (26
230 out of 27) and thiamine pyrophosphate (5 out of 6) (Bunik et al., 2016). Pair-wise alignments
231 allowed us to generate a phylogenetic tree (Fig. 1B). Amongst fish, *S. aurata* GDH exhibited higher
232 similarity with sequences reported for *Lates calcarifer*, *Nothobranchius furzeri*, *Paralichthys*
233 *olivaceus* and *Xiphophorus maculatus* (96.3-97.1 % of identity). A lower identity was observed
234 when compared to *Salmo salar* (92.6 %) and *Danio rerio* (87.5 %). Concerning mammalian
235 orthologues, *S. aurata* GDH shared 81.2 to 84.3 % identity with *Mus musculus*, *Rattus norvegicus*
236 and *Homo sapiens* GDH.
237
238 *3.2. Validation of shRNA expression constructs to silence* S. aurata *GDH in HepG2 cells*
239 Five shRNA (named sh1 to sh5) designed to knockdown *S. aurata* GDH were subcloned into
240 pCpG-siRNA, a vector that allows long lasting expression of small interfering RNA (siRNA) *in*
241 *vivo*. Efficiency of GDH silencing for the resulting constructs (pCpG-sh1GDH to pCpG-sh5GDH)
242 was validated in HepG2 cells co-transfected with 30 ng or 300 ng of a construct expressing *S.*
243 *aurata* GDH (pcDNA3-GDH), 300 ng of pCMV-β and 600 ng of pCpG-sh1GDH, pCpG-sh2GDH,
244 pCpG-sh3GDH, pCpG-sh4GDH, pCpG-sh5GDH or pCpG-siRNA-Scramble (control). Forty-eight
245 hours later, the cells were lysed and RNA isolated to perform RT-qPCR assays to determine *S.*
246 *aurata* GDH mRNA levels. Three shRNAs (sh2, sh3 and sh5) significantly decreased GDH
247 expression in HepG2 cells co-transfected with 30 ng of pcDNA3-GDH, while sh2 was the only that
248 significantly down-regulated GDH mRNA in the cells co-transfected with a higher concentration of
249 pcDNA3-GDH (300 ng). In all cases, the highest GDH gene silencing effect was observed with sh2,
250 which reduced values to 21 % and 55 % of controls (Scramble) after co-tranfection with 30 ng and

251 300 ng of pcDNA3-GDH, respectively (Fig. 2A). Therefore, sh2 was selected for subsequent
252 studies.
253
254 *3.3. Effect of chitosan-TPP-pCpG-sh2GDH administration on GDH expression in the liver of* S.
255 aurata
256 To study the metabolic effects of GDH silencing, chitosan-TPP nanoparticles were complexed
257 with pCpG-sh2GDH to deliver and express sh2 into *S. aurata* liver cells. Schematic representation
258 of chitosan-TPP-DNA nanoparticles is shown in Figure 2B. Atomic force microscopy on chitosan-
259 TPP nanoparticles showed a rounded morphology with mean diameter size ± SD (n=6) of 224.0 nm
260 ± 62.4 (Fig. 2C), and presented a mean *Z* potential of 32.98 mV ± 1.16. Incorporation of pCpG-
261 siRNA constructs to chitosan-TPP nanoparticles did not significantly affect morphology or mean
262 diameter size, while reduced mean *Z* potential to 14.37 mV ± 1.29. Three groups of fish received an
263 intraperitoneal injection of chitosan-TPP-pCpG-sh2GDH (10 μg of plasmid/g BW), chitosan-TPP-
264 pCpG-siRNA-Scramble (10 μg of plasmid/g BW; negative control) or chitosan-TPP nanoparticles
265 (negative control of chitosan-TPP not complexed with DNA). GDH mRNA levels,
266 immunodetectable protein and enzyme activity were determined in the liver at 72 hours post-
267 treatment. As expected, inclusion of pCpG-siRNA-Scramble into chitosan-TPP nanoparticles did
268 not affect GDH mRNA levels in the liver. However, administration of chitosan-TPP-pCpG-
269 sh2GDH significantly decreased GDH expression to 41 % of control values (Scramble) (Fig. 2B).
270 Consistent with sh2-mediated down-regulation of GDH mRNA, treatment with pCpG-sh2GDH
271 decreased immunodetectable GDH protein in liver extracts and decreased GDH activity in both
272 oxidative and reductive reactions to about 53-55 % of control values (Fig. 3A).
273
274 *3.4 Effect of GDH knockdown on the hepatic intermediary metabolism of* S. aurata

275 The effect of GDH silencing was also studied on hepatic key enzyme activities involved in
276 amino acid metabolism, glycolysis-gluconeogenesis and the Krebs cycle, 2-oxoglutarate levels and
277 amino acid profile. In regard of amino acid metabolism, knockdown of GDH significantly
278 decreased AST activity to about 73 % of control levels. Albeit not significant, the same trend was
279 observed for ALT (Fig. 3B). We also addressed the effect of GDH silencing on PFK and FBP1
280 activity, which exert a major role in glucose homeostasis by controlling the flux through the
281 fructose-6-phosphate/fructose-1,6-bisphosphate substrate cycle. GDH knockdown did not affect
282 PFK activity, but significantly reduced FBP1 activity to 63 % of controls. Therefore, the PFK/FBP1
283 ratio increased to 122 % as a result of GDH silencing (Fig. 3C). The hepatic content of 2-
284 oxoglutarate, a substrate of the reductive GDH reaction, significantly increased to 172 % in the liver
285 of fish treated with chitosan-TPP-pCpG-sh2GDH. Given that 2-oxoglutarate is also a substrate of
286 OGDH, a rate-limiting complex of the Krebs cycle, we analysed OGDH activity in the liver. GDH
287 silencing increased OGDH activity to 135 % (Fig. 3D). Since GDH has a major role in liver amino
288 acid catabolism through oxidative deamination of L-glutamate, changes in amino acid and related
289 molecules profile resulting from GDH silencing were also determined. Administration of chitosan-
290 TPP-pCpG-sh2GDH nanoparticles significantly decreased glutamate and glutamine to 80 % and 64
291 % of their respective controls. GDH silencing also decreased α-aminobutyric acid to 76 % of
292 control values, while increased 1.2-fold methionine levels (Table 2).
293

294 **4. Discussion**

295 Teleost fish use efficiently amino acids for growth and to obtain energy, while exhibit slower
296 dietary carbohydrate digestion and free sugar metabolisation than mammals, giving rise to
297 prolonged hyperglycemia. Therefore, optimal growth of fish requires high levels of dietary protein
298 (Moon, 2001; Polakof et al., 2012). However, a reduction in the amount of protein in aquafeeds
299 would alleviate dependence on wild fisheries and the environmental impact of aquaculture (Gormaz

300 et al., 2014; Martinez-Porchas and Martinez-Cordova, 2012; Naylor et al., 2000). The main site of
301 amino acid catabolism is the liver and primarily involves transdeamination, in which the amino
302 group of a variety of amino acids is transferred to 2-oxoglutarate to produce glutamate, which in
303 turn can be deaminated by GDH. The fact that the molecular role of GDH in fish remains largely
304 unexplored prompted us to study the effect of GDH silencing on *S. aurata* liver intermediary
305 metabolism. To this end, the full length GDH cDNA sequence from *S. aurata* was isolated. As
306 expected, alignment of the inferred peptide sequence of *S. aurata* GDH with those reported for
307 other fish species gave the highest identity (>96 %) with species from the *Percomorphaceae*
308 subdivision (*Lates calcarifer*, *Nothobranchius furzeri*, *Paralichthys olivaceus* and *Xiphophorus*
309 *maculatus*), the subdivision to which *S. aurata* belongs. A slightly lower identity was found when
310 compared to phylogenetically distant fish species, such as *Salmoniformes* (*Salmo salar*) and
311 *Cypriniformes* (*Danio rerio*).

312 *S. aurata* GDH retains all residues involved in glutamate binding and GTP inhibition (31 in
313 total), and most of the residues considered of importance for NAD^+ and thiamine pyrophosphate
314 binding, and ADP activation (51 out of 58) (Bunik et al., 2016). Indeed, analysis of non-conserved
315 amino acids involved in catalysis and allosteric regulation of GDH reveals that 6 out of 7 are
316 conservative mutations. The only significant difference between species from the *Percomorphaceae*
317 subdivision (including *S. aurata*) and mammalian GDH resides in the substitution of a serine
318 residue involved in NAD^+ binding by Gly368 in *S. aurata* GDH. Taken together, the overall
319 similarity with mammalian GDH suggests a high degree of conservation of the structure and
320 conceivably the reaction mechanism during vertebrate evolution.

321 Availability of *S. aurata* GDH cDNA sequence allowed us to design shRNAs to knockdown
322 GDH expression and analyse the metabolic effects derived from GDH silencing. Validation of five
323 selected shRNAs was performed in HepG2 cells co-transfected with shRNA and *S. aurata* GDH
324 expression plasmids. The most effective shRNA *in vitro* (sh2) was subsequently chosen to evaluate

325 metabolic effects of GDH gene silencing *in vivo*. As a vector to deliver pCpG-sh2GDH (sh2
326 expression plasmid) into *S. aurata* hepatocytes, we used chitosan, which is a cationic polymer
327 composed of glucosamine and N-acetylglucamosine, derived from chitin by deacetylation.
328 Mucoadhesion, low toxicity, biodegradability and biocompatibility of chitosan led in recent years to
329 increasing use of chitosan as a carrier to facilitate incorporation of DNA constructs into host cells *in*
330 *vivo* (Ragelle et al., 2014; Sáez et al., 2017). Recently, administration of chitosan-TPP-DNA
331 nanoparticles to knockdown *S. aurata* cytosolic ALT allowed us to demonstrate that cytosolic ALT
332 silencing enhanced rate-limiting activities of glycolysis, while did not affect gluconeogenesis
333 (González et al., 2016). Based on this methodology, in the present study we used the ionic gelation
334 technique, a method based on interactions between low molecular weight chitosan and polyanions
335 such as TPP (Fàbregas et al., 2013), to encapsulate pCpG-sh2GDH and analyse the effect of GDH
336 silencing on the hepatic metabolism of *S. aurata*. Seventy-two hours following intraperitoneal
337 administration of chitosan-TPP-pCpG-sh2GDH, the hepatic expression of GDH was significantly
338 reduced at mRNA level, immunodetectable protein and reductive and oxidative enzyme activity. No
339 sickness, death or behavioural alterations were observed as a consequence of GDH silencing.
340 Similarly as in *S. aurata*, previous studies showed that although GDH deletion leads to deficient
341 oxidative metabolism of glutamate in the central nervous system, brain-specific Glud1 null mice
342 were viable, fertile and without apparent behavioural problems (Frigerio et al., 2012).

343 Consistent with the liver as the main site for GDH expression, GDH silencing promoted
344 significant changes on the hepatic levels of GDH substrates and products: glutamate and 2-
345 oxoglutarate. As a result of GDH silencing, 2-oxoglutarate levels increased in the liver of *S. aurata*.
346 Elevated 2-oxoglutarate values may determine enhancement of OGDH activity, a key enzyme
347 complex of the Krebs cycle. In agreement with increased 2-oxoglutarate levels, a decreased GDH
348 activity led to the opposite effects on the hepatic content of glutamate. Since 2-oxoglutarate can be
349 converted to glutamate by either GDH or transaminases, it is conceivable that low glutamate levels
350 were reinforced by inhibition of ALT and AST, which are considered the more relevant

351 aminotransferases in the liver. Altogether, our findings point to decreased transaminase activity and
352 reduced transdeamination resulting from GDH silencing in the *S. aurata* liver. Indeed, given that
353 glutamine synthetase can synthesise glutamine from glutamate, the low levels of glutamate may be
354 responsible for decreased glutamine values in the liver of fish treated with chitosan-TPP-pCpG-
355 sh2GDH.

356 Bearing in mind that methionine is an essential amino acid in animals, the fact that
357 methionine levels were higher in the liver of fish treated with chitosan-TPP-pCpG-sh2GDH
358 nanoparticles suggests that GDH silencing decreased methionine metabolism, which in turn may
359 result in reduced α-aminobutyric acid levels. Considering that it was recently reported that high
360 protein diets increase α-aminobutyric acid in humans (Haschke-Becher et al., 2016), the low levels
361 of α-aminobutyric acid in the liver of treated fish can also be a consequence of decreased amino
362 acid metabolism as a result of GDH silencing.

363 In a context with reduced transdeaminating capacity, the use of amino acids as glucogenic and
364 ketogenic substrates, and to produce energy by entering catabolic pathways, could be compromised.
365 In this regard, it is remarkable that GDH knockdown increased PFK/FBP1 activity ratio, which
366 suggests that glycolysis was favoured over gluconeogenesis in the liver of treated fish. This
367 metabolic shift could enhance the use of dietary carbohydrates as fuel for energy production as a
368 compensatory mechanism resulting from impaired transdeamination and reduced entrance of the
369 carbon skeleton of amino acids into the Krebs cycle to obtain energy and as gluconeogenic
370 substrates. Our findings are consistent with increased glucose utilisation in cultured mice astrocytes
371 treated with siRNA to knockdown GDH expression (Pajęcka et al., 2015). The authors concluded
372 that glucose could replace glutamate as energy substrate in GDH-deficient cells on the basis that
373 siRNA-treated astrocytes were able to maintain physiological levels of ATP regardless of GDH
374 expression by increasing glucose oxidation. Furthermore, consistent with the rise in OGDH
375 complex activity and elevated 2-oxoglutarate levels in the liver of *S. aurata* treated with chitosan-

376 TPP-pCpG-sh2GDH nanoparticles, GDH deficient astrocytes exhibit an increased glucose
377 metabolism linked to elevated Krebs cycle flux from 2-oxoglutarate to oxaloacetate and up-
378 regulation of anaplerotic pathways such as pyruvate carboxylase to maintain the amount of Krebs
379 cycle intermediates (Nissen et al., 2015). Indeed, transgenic mice expressing human GDH2 showed
380 a general decrease in oxidative glucose metabolism (Nissen et al., 2017).

381 By hindering the use of amino acids as gluconeogenic substrates and favouring glucose
382 oxidation in the liver of *S. aurata*, GDH silencing may enable partial substitution of dietary protein
383 by carbohydrates in aquafeeds. Fishmeal is the main protein source in fish farming and it is
384 obtained by processing an important part of wild fish captures. Therefore, a reduction in the amount
385 of protein in aquafeeds would alleviate dependence on wild fisheries and decrease local
386 eutrophication resulting from amino acid oxidation and ammonia release of excess dietary protein.
387 In addition to reduce environmental impact of aquaculture, substitution of dietary protein by
388 cheaper nutrients such as carbohydrates, would decrease production costs.

389 In conclusion, we addressed the metabolic effects of GDH silencing in the liver of *S. aurata*.
390 Data presented suggest that knockdown of GDH expression reduces hepatic transdeamination and
391 compromises the use of amino acids as gluconeogenic substrates. Our findings point to GDH
392 silencing as a target to spare protein, stimulate glucose metabolism and reduce environmental
393 impact and production costs of aquaculture through partial substitution of dietary protein by
394 carbohydrates.

395

396 **Acknowledgements**

397 This work was supported by the Ministerio de Economía, Industria y Competitividad of Spain
398 (grant number AGL2016-78124-R; cofunded by the European Regional Development Fund,
399 European Comission). The authors thank Piscimar (Burriana, Castellón, Spain) for providing *S.*
400 *aurata* juveniles, and the Aquarium of Barcelona (Barcelona, Spain) for supplying filtered seawater.

401

402 **Declarations of interest:** none.

403

404 **References**

405 Bibiano Melo, J.F., Lundstedt, L.M., Metón, I., Baanante, I.V., Moraes, G., 2006. Effects of dietary
406 levels of protein on nitrogenous metabolism of Rhamdia quelen (Teleostei: Pimelodidae).
407 Comp. Biochem. Physiol. A Mol. Integr. Physiol. 145, 181–187.

408 Borges, P., Medale, F., Dias, J., Valente, L.M.P., 2013. Protein utilisation and intermediary
409 metabolism of Senegalese sole (Solea senegalensis) as a function of protein:lipid ratio. Br. J.
410 Nutr. 109, 1373–1381.

411 Bunik, V., Artiukhov, A., Aleshin, V., Mkrtchyan, G., 2016. Multiple Forms of Glutamate
412 Dehydrogenase in Animals: Structural Determinants and Physiological Implications. Biology
413 5, 53.

414 Caballero-Solares, A., Viegas, I., Salgado, M.C., Siles, A.M., Sáez, A., Metón, I., Baanante, I.V.,
415 Fernández, F., 2015. Diets supplemented with glutamate or glutamine improve protein
416 retention and modulate gene expression of key enzymes of hepatic metabolism in gilthead
417 seabream (Sparus aurata) juveniles. Aquaculture 444, 79–87.

418 Carobbio, S., Frigerio, F., Rubi, B., Vetterli, L., Bloksgaard, M., Gjinovci, A.,
419 Pournourmohammadi, S., Herrera, P.L., Reith, W., Mandrup, S., Maechler, P., 2009. Deletion
420 of glutamate dehydrogenase in beta-cells abolishes part of the insulin secretory response not
421 required for glucose homeostasis. J. Biol. Chem. 284, 921–929.

422 Carobbio, S., Ishihara, H., Fernandez-Pascual, S., Bartley, C., Martin-Del-Rio, R., Maechler, P.,
423 2004. Insulin secretion profiles are modified by overexpression of glutamate dehydrogenase in
424 pancreatic islets. Diabetologia 47, 266–276.

425 Chevenet, F., Brun, C., Bañuls, A.-L., Jacq, B., Christen, R., 2006. TreeDyn: towards dynamic

426 graphics and annotations for analyses of trees. BMC Bioinformatics 7, 439.
427 Coutinho, F., Peres, H., Castro, C., Pérez-Jiménez, A., Pousão-Ferreira, P., Oliva-Teles, A., Enes,
428 P., 2016. Metabolic responses to dietary protein/carbohydrate ratios in zebra sea bream
429 (Diplodus cervinus, Lowe, 1838) juveniles. Fish Physiol. Biochem. 42, 343–352.
430 Couto, A., Enes, P., Peres, H., Oliva-Teles, A., 2008. Effect of water temperature and dietary starch
431 on growth and metabolic utilization of diets in gilthead sea bream (Sparus aurata) juveniles.
432 Comp. Biochem. Physiol. A Mol. Integr. Physiol. 151, 45–50.
433 Emanuelsson, O., Nielsen, H., Brunak, S., von Heijne, G., 2000. Predicting Subcellular Localization
434 of Proteins Based on their N-terminal Amino Acid Sequence. J. Mol. Biol. 300, 1005–1016.
435 Fàbregas, A., Miñarro, M., García-Montoya, E., Pérez-Lozano, P., Carrillo, C., Sarrate, R.,
436 Sánchez, N., Ticó, J.R., Suñé-Negre, J.M., 2013. Impact of physical parameters on particle size
437 and reaction yield when using the ionic gelation method to obtain cationic polymeric chitosan-
438 tripolyphosphate nanoparticles. Int. J. Pharm. 446, 199–204.
439 Fernández, F., Miquel, A.G., Cordoba, M., Varas, M., Metón, I., Caseras, A., Baanante, I.V., 2007.
440 Effects of diets with distinct protein-to-carbohydrate ratios on nutrient digestibility, growth
441 performance, body composition and liver intermediary enzyme activities in gilthead sea bream
442 (Sparus aurata, L.) fingerlings. J. Exp. Mar. Bio. Ecol. 343, 1–10.
443 Frick, N.T., Bystriansky, J.S., Ip, Y.K., Chew, S.F., Ballantyne, J.S., 2008. Carbohydrate and amino
444 acid metabolism in fasting and aestivating African lungfish (Protopterus dolloi). Comp.
445 Biochem. Physiol. A Mol. Integr. Physiol. 151, 85–92.
446 Frigerio, F., Karaca, M., De Roo, M., Mlynárik, V., Skytt, D.M., Carobbio, S., Pajęcka, K.,
447 Waagepetersen, H.S., Gruetter, R., Muller, D., Maechler, P., 2012. Deletion of glutamate
448 dehydrogenase 1 (Glud1) in the central nervous system affects glutamate handling without
449 altering synaptic transmission. J Neurochem. 123, 342–348.
450 Gaspar, C., Silva-Marrero, J.I., Salgado, M.C., Baanante, I.V., Metón, I., 2018. Role of upstream

451 stimulatory factor 2 in glutamate dehydrogenase gene transcription. J. Mol. Endocrinol., in
452 press. doi:10.1530/JME-17-0142.
453 Göhring, I., Mulder, H., 2012. Glutamate dehydrogenase, insulin secretion, and type 2 diabetes: a
454 new means to protect the pancreatic β-cell? J. Endocrinol. 212, 239–242.
455 González, J.D., Silva-Marrero, J.I., Metón, I., Caballero-Solares, A., Viegas, I., Fernández, F.,
456 Miñarro, M., Fàbregas, A., Ticó, J.R., Jones, J.G., Baanante, I.V., 2016. Chitosan-Mediated
457 shRNA Knockdown of Cytosolic Alanine Aminotransferase Improves Hepatic Carbohydrate
458 Metabolism. Mar. Biotechnol. 18, 85–97.
459 Gormaz, J.G., Fry, J.P., Erazo, M., Love, D.C., 2014. Public Health Perspectives on Aquaculture.
460 Curr. Environ. Heal. Reports 1, 227–238.
461 Graham, F.L., van der Eb, A.J., 1973. A new technique for the assay of infectivity of human
462 adenovirus 5 DNA. Virology 52, 456–467.
463 Guindon, S., Dufayard, J.-F., Lefort, V., Anisimova, M., Hordijk, W., Gascuel, O., 2010. New
464 Algorithms and Methods to Estimate Maximum-Likelihood Phylogenies: Assessing the
465 Performance of PhyML 3.0. Syst. Biol. 59, 307–321.
466 Haschke-Becher, E., Kainz, A., Bachmann, C., 2016. Reference values of amino acids and of
467 common clinical chemistry in plasma of healthy infants aged 1 and 4 months. J. Inherit. Metab.
468 Dis. 39, 25–37.
469 Karaca, M., Frigerio, F., Maechler, P., 2011. From pancreatic islets to central nervous system, the
470 importance of glutamate dehydrogenase for the control of energy homeostasis. Neurochem.
471 Int. 59, 510–517.
472 Li, M., Li, C., Allen, A., Stanley, C.A., Smith, T.J., 2014. Glutamate dehydrogenase: structure,
473 allosteric regulation, and role in insulin homeostasis. Neurochem. Res. 39, 433–445.
474 Lushchak, V.I., Husak, V. V, Storey, K.B., 2008. Regulation of AMP-deaminase activity from
475 white muscle of common carp Cyprinus carpio. Comp. Biochem. Physiol. B. Biochem. Mol.

476 Biol. 149, 362–369.
477 Martinez-Porchas, M., Martinez-Cordova, L.R., 2012. World aquaculture: environmental impacts
478 and troubleshooting alternatives. Sci. World J. 2012, 389623.
479 Metón, I., Egea, M., Anemaet, I.G., Fernández, F., Baanante, I.V., 2006. Sterol regulatory element
480 binding protein-1a transactivates 6-phosphofructo-2-kinase/fructose-2,6-bisphosphatase gene
481 promoter. Endocrinology 147, 3446–3456.
482 Metón, I., Mediavilla, D., Caseras, A., Cantó, E., Fernández, F., Baanante, I.V., 1999. Effect of diet
483 composition and ration size on key enzyme activities of glycolysis-gluconeogenesis, the
484 pentose phosphate pathway and amino acid metabolism in liver of gilthead sea bream (Sparus
485 aurata). Br. J. Nutr. 82, 223–232.
486 Moon, T.W., 2001. Glucose intolerance in teleost fish: fact or fiction? Comp. Biochem. Physiol. B
487 Biochem. Mol. Biol. 129, 243–249.
488 Moore, S., Spackman, D.H., Stein, W.H., 1958. Automatic recording apparatus for use in the
489 chromatography of amino acids. Fed. Proc. 17, 1107–1115.
490 Naylor, R.L., Goldburg, R.J., Primavera, J.H., Kautsky, N., Beveridge, M.C., Clay, J., Folke, C.,
491 Lubchenco, J., Mooney, H., Troell, M., 2000. Effect of aquaculture on world fish supplies.
492 Nature 405, 1017–1024.
493 Nielsen, H., Engelbrecht, J., Brunak, S., von Heijne, G., 1997. Identification of prokaryotic and
494 eukaryotic signal peptides and prediction of their cleavage sites. Protein Eng. 10, 1–6.
495 Nissen, J.D., Lykke, K., Bryk, J., Stridh, M.H., Zaganas, I., Skytt, D.M., Schousboe, A., Bak, L.K.,
496 Enard, W., Pääbo, S., Waagepetersen, H.S., 2017. Expression of the human isoform of
497 glutamate dehydrogenase, hGDH2, augments TCA cycle capacity and oxidative metabolism of
498 glutamate during glucose deprivation in astrocytes. Glia 65, 474–488.
499 Nissen, J.D., Pajęcka, K., Stridh, M.H., Skytt, D.M., Waagepetersen, H.S., 2015. Dysfunctional
500 TCA-Cycle Metabolism in Glutamate Dehydrogenase Deficient Astrocytes. Glia 63, 2313–

501 2326.
502 Pajęcka, K., Nissen, J.D., Stridh, M.H., Skytt, D.M., Schousboe, A., Waagepetersen, H.S., 2015.
503 Glucose replaces glutamate as energy substrate to fuel glutamate uptake in glutamate
504 dehydrogenase-deficient astrocytes. J. Neurosci. Res. 93, 1093–1100.
505 Peres, H., Oliva-Teles, A., 2006. Protein and Energy Metabolism of European Seabass
506 (Dicentrarchus labrax) Juveniles and Estimation of Maintenance Requirements. Fish Physiol.
507 Biochem. 31, 23–31.
508 Pérez-Jiménez, A., Cardenete, G., Hidalgo, M.C., García-Alcázar, A., Abellán, E., Morales, A.E.,
509 2012. Metabolic adjustments of Dentex dentex to prolonged starvation and refeeding. Fish
510 Physiol. Biochem. 38, 1145–1157.
511 Pérez-Jiménez, A., Guedes, M.J., Morales, A.E., Oliva-Teles, A., 2007. Metabolic responses to
512 short starvation and refeeding in Dicentrarchus labrax. Effect of dietary composition.
513 Aquaculture 265, 325–335.
514 Pfaffl, M.W., 2001. A new mathematical model for relative quantification in real-time RT-PCR.
515 Nucleic Acids Res. 29, e45.
516 Plaitakis, A., Kalef-Ezra, E., Kotzamani, D., Zaganas, I., Spanaki, C., 2017. The Glutamate
517 Dehydrogenase Pathway and Its Roles in Cell and Tissue Biology in Health and Disease.
518 Biology 6, 11.
519 Polakof, S., Panserat, S., Soengas, J.L., Moon, T.W., 2012. Glucose metabolism in fish: a review. J.
520 Comp. Physiol. B 182, 1015–1045.
521 Ragelle, H., Riva, R., Vandermeulen, G., Naeye, B., Pourcelle, V., Le Duff, C.S., D'Haese, C.,
522 Nysten, B., Braeckmans, K., De Smedt, S.C., Jérôme, C., Préat, V., 2014. Chitosan
523 nanoparticles for siRNA delivery: optimizing formulation to increase stability and efficiency.
524 J. Control. Release 176, 54–63.
525 Sáez, M., Vizcaíno, A., Alarcón, F., Martínez, T., 2017. Comparison of lacZ reporter gene

526 expression in gilthead sea bream (Sparus aurata) following oral or intramuscular
527 administration of plasmid DNA in chitosan nanoparticles. Aquaculture 474, 1–10.
528 Sánchez-Muros, M.J., García-Rejón, L., García-Salguero, L., de la Higuera, M., Lupiáñez, J.A.,
529 1998. Long-term nutritional effects on the primary liver and kidney metabolism in rainbow
530 trout. Adaptive response to starvation and a high-protein, carbohydrate-free diet on glutamate
531 dehydrogenase and alanine aminotransferase kinetics. Int. J. Biochem. Cell Biol. 30, 55–63.
532 Sievers, F., Wilm, A., Dineen, D., Gibson, T.J., Karplus, K., Li, W., Lopez, R., McWilliam, H.,
533 Remmert, M., Söding, J., Thompson, J.D., Higgins, D.G., 2011. Fast, scalable generation of
534 high-quality protein multiple sequence alignments using Clustal Omega. Mol. Syst. Biol. 7,
535 539.
536 Tian, J., He, G., Mai, K., Liu, C., 2015. Effects of postprandial starvation on mRNA expression of
537 endocrine-, amino acid and peptide transporter-, and metabolic enzyme-related genes in
538 zebrafish (Danio rerio). Fish Physiol. Biochem. 41, 773–787.
539 Tranulis, M.A., Christophersen, B., Blom, A.K., Borrebaek, B., 1991. Glucose dehydrogenase,
540 glucose-6-phosphate dehydrogenase and hexokinase in liver of rainbow trout (Salmo
541 gairdneri). Effects of starvation and temperature variations. Comp. Biochem. Physiol. B 99,
542 687–691.
543 Treberg, J.R., Banh, S., Pandey, U., Weihrauch, D., 2014. Intertissue differences for the role of
544 glutamate dehydrogenase in metabolism. Neurochem. Res. 39, 516–526.
545 Viegas, I., Rito, J., Jarak, I., Leston, S., Caballero-Solares, A., Metón, I., Pardal, M.A., Baanante,
546 I.V., Jones, J.G., 2015. Contribution of dietary starch to hepatic and systemic carbohydrate
547 fluxes in European seabass (Dicentrarchus labrax L.). Br. J. Nutr. 113, 1345–1354.
548
549 **Figure captions**

550 **Fig. 1.** Multiple alignment and phylogenetic tree of GDH. (A) Alignment of the predicted amino
551 acid sequence of *S. aurata* GDH with GDH orthologues in other vertebrates. Black, identical amino
552 acids; grey, conservative amino acid substitutions. Letters on the top indicate residues involved in
553 the binding to ADP (A), glutamate (E), GTP (G), NAD^+ (N) and thiamine pyrophosphate (T).
554 GenBank entries shown are: *Sparus aurata* (**MF459045**); *Nothobranchius furzeri* (**XP_015818399**);
555 *Xiphophorus maculatus* (**XP_005794695**); *Lates calcarifer* (**XP_018531054**), *Paralichthys*
556 *olivaceus* (**XP_019938702**), *Salmo salar* (**NP_001117108**), *Danio rerio* (**NP_997741**), *Mus*
557 *musculus* GDH1 (**NP_032159**), *Rattus norvegicus* GDH1 (**NP_036702**), *Homo sapiens* GDH1
558 (**NP_005262**) and *Homo sapiens* GDH2 (**NP_036216**). (B) Phylogenetic tree for GDH. Multiple
559 alignment and phylogenetic tree were made with Clustal Omega (Sievers et al., 2011), PhyML
560 (Guindon et al., 2010), and TreeDyn (Chevenet et al., 2006).
561
562 **Fig. 2.** *In vitro* validation of shRNA-mediated silencing of *S. aurata* GDH and effect of chitosan-
563 TPP-DNA nanoparticles on hepatic GDH mRNA levels in *S. aurata*. (A) HepG2 cells were co-
564 transfected with of pcDNA3-GDH (30 ng or 300 ng), pCMV-β (300 ng) and pCpG-sh1GDH,
565 pCpG-sh2GDH, pCpG-sh3GDH, pCpG-sh4GDH or pCpG-sh5GDH (600 ng). *S. aurata* GDH
566 mRNA levels at 48 hours post-transfection were analysed by RT-qPCR and normalised with human
567 ribosomal subunit 18s and β-galactosidase (internal control of transfection). (B) Molecular structure
568 and electrostatic interactions of chitosan-TPP-DNA nanoparticles. (C) The left part of the panel
569 shows representative images of chitosan-TPP, chitosan-TPP-pCpG-siRNA-Scramble and chitosan-
570 TPP-pCpG-sh2GDH nanoparticles obtained by atomic force microscopy. White bars correspond to
571 200 nm. The right part of the panel shows the effect of nanoparticle administration on GDH mRNA
572 levels in the *S. aurata* liver. Three groups of fish were intraperitoneally injected with chitosan-TPP
573 (Chitosan), chitosan-TPP-pCpG-siRNA-Scramble (Scramble; 10 μg of plasmid/g BW) or chitosan-
574 TPP-pCpG-sh2GDH (sh2; 10 μg of plasmid/g BW). Analysis of GDH mRNA levels relative to the

575 geometric mean of ribosomal subunit 18s, β-actin and EF1α were performed by RT-qPCR in liver
576 samples of *S. aurata* at 72 hours post-treatment. The values are expressed as mean ± SD (n=4, *in*
577 *vitro* analysis; n=6, *in vivo* analysis). Statistical significance related to control (Scramble) is
578 indicated as follows: $^{**}P < 0.01$; $^{***}P < 0.001$.

579

580 **Fig. 3.** Effect of chitosan-TPP-DNA nanoparticles on GDH protein and activity, 2-oxoglutarate
581 content and key enzyme activities in the *S. aurata* liver metabolism. (A) Effect of GDH silencing on
582 immunodetectable GDH protein, shown as a representative Western blot (upper part of the panel),
583 and reductive and oxidative GDH activity (lower part of the panel). (B) Effect of GDH silencing on
584 ALT and AST activity. (C) Effect of GDH silencing on PFK and FBP1 activity, and PFK/FBP1
585 activity ratio. (D) Effect of GDH silencing on 2-oxoglutarate levels and OGDH activity. GDH
586 immunodetectable protein, enzyme activities and 2-oxoglutarate content were assayed in liver crude
587 extracts 72 hours after administration of 10 μg/g BW of pCpG-siRNA-Scramble (Scramble) or
588 chitosan-TPP-pCpG-sh2GDH (sh2). 2-Oxoglutarate concentration and enzyme specific activities
589 are expressed as mean ± SD (n=6). Statistical significance related to control (Scramble) is indicated
590 as follows: $^{*}P < 0.05$; $^{**}P < 0.01$.

591 **Table 1.** Oligonucleotides used in the present study.

Primer	Sequence (5' to 3')
CG1305	ACTTGAATGCTGGTGGTGTGACAGTGT
CG1306	CCCACCACCCCAGATGCTGACAAGAT
CG1307	GTCTTGTCCTGGAAGCCTGGTGTCA
CG1308	GGCTGAGATACGACCGTGGATACCTCCC
CG1333	TTCCTTAAACACAATTTCAACGTCAA
CG1334	GGAGCTGCTGTGTCGTTCAT
CG1526	CCGGATCCACCATGGACCGGTATTTCGGGGAG
CG1527	CCGAATTCGGCTGTTTAGAGGGGGGAGAATAG
CG1531	GTACCTCGTTCGTTTACACGGTTAGCTATCAAGAGTAGCTAACCGTG TAAACGAACTTTTTGGAAA
CG1532	AGCTTTTCCAAAAAGTTCGTTTACACGGTTAGCTACTCTTGATAGCT AACCGTGTAAACGAACGAG
CG1533	GTACCTCGCGCATCATCAAGCCCTGTAATCAAGAGTTACAGGGCTTG ATGATGCGCTTTTTGGAAA
CG1534	AGCTTTTCCAAAAAGCGCATCATCAAGCCCTGTAACTCTTGATTACA GGGCTTGATGATGCGCGAG
CG1535	GTACCTCGAGCCAAAGCTGGAGTCAAGATCAAGAGTCTTGACTCCA GCTTTGGCTCTTTTTGGAAA
CG1536	AGCTTTTCCAAAAAGAGCCAAAGCTGGAGTCAAGACTCTTGATCTTG ACTCCAGCTTTGGCTCGAG
CG1537	GTACCTCGAGAACAACGTCATGGTTATTTCAAGAGAATAACCATGAC GTTGTTCTCTTTTTGGAAA

CG1538	AGCTTTTCCAAAAAGAGAACAACGTCATGGTTATTCTCTTGAAATAA CCATGACGTTGTTCTCGAG
CG1539	GTACCTCGGCTGGACTTACCTTCACATATCAAGAGTATGTGAAGGTA AGTCCAGCCTTTTTGGAAA
CG1540	AGCTTTTCCAAAAAGGCTGGACTTACCTTCACATACTCTTGATATGT GAAGGTAAGTCCAGCCGAG
CG1543	GGTATTTCGGGGAGCTGCTGAG
CG1544	CGCATCAGGGACGAGGACA
AS-EF1Fw	CCCGCCTCTGTTGCCTTCG
AS-EF1Rv	CAGCAGTGTGGTTCCGTTAGC
JDRT18S	TTACGCCCATGTTGTCCTGAG
JDRT18AS	AGGATTCTGCATGATGGTCACC
JDRTCMVBS	CCCATTACGGTCAATCCGC
JDRTCMVBAS	ACAACCCGTCGGATTCTCC
QBACTINF	CTGGCATCACACCTTCTACAACGAG
QBACTINR	GCGGGGGTGTTGAAGGTCTC

The following primers contain restriction sites (*underlined*): CG1526 (*Bam*HI) and CG1527 (*Eco*RI).

595 **Table 2.** Effect of GDH silencing on the hepatic levels of amino acids and related molecules.

Metabolite	Scramble (nmol/mg liver)	sh2 (nmol/mg liver)
Taurine	11.96±0.57	12.18±0.80
Urea	2.78±0.45	2.77±0.35
Aspartate	1.90±0.15	2.09±0.17
Threonine	2.54±0.10	3.08±0.68
Serine	0.37±0.04	0.36±0.13
Asparagine	0.28±0.13	0.29±0.11
Glutamate	5.37±0.53	4.30*±0.40
Glutamine	1.46±0.16	0.94**±0.05
Sarcosine	6.89±1.42	6.48±0.86
Proline	0.52±0.21	0.71±0.08
Glycine	2.33±0.39	2.57±0.54
Alanine	7.94±1.18	7.95±0.70
α-Aminobutyric acid	0.16±0.02	0.12*±0.03
Valine	0.14±0.02	0.18±0.03
Methionine	0.13±0.02	0.16*±0.02
Cystathionine	0.51±0.09	0.59±0.33
Isoleucine	0.13±0.01	0.11±0.01
Leucine	0.20±0.02	0.21±0.03
Tyrosine	0.06±0.01	0.06±0.02
β-Alanine	0.44±0.19	0.41±0.15
Phenylalanine	0.10±0.02	0.12±0.01

Ornithine	0.07±0.02	0.07±0.03
Lysine	0.40±0.07	0.57±0.15
Histidine	0.46±0.08	0.56±0.08
Arginine	0.20±0.03	0.24±0.06

596

597 Metabolites were assayed in liver extracts 72 hours following administration of 10 μg of pCpG-
598 siRNA-Scramble (Scramble) or chitosan-TPP-pCpG-sh2GDH (sh2) per gram BW. The values are
599 expressed as mean ± SD (n=5). Statistical significance related to control fish (Scramble) is indicated
600 as follows: *$P < 0.05$; **$P < 0.01$.

Figure 1

A

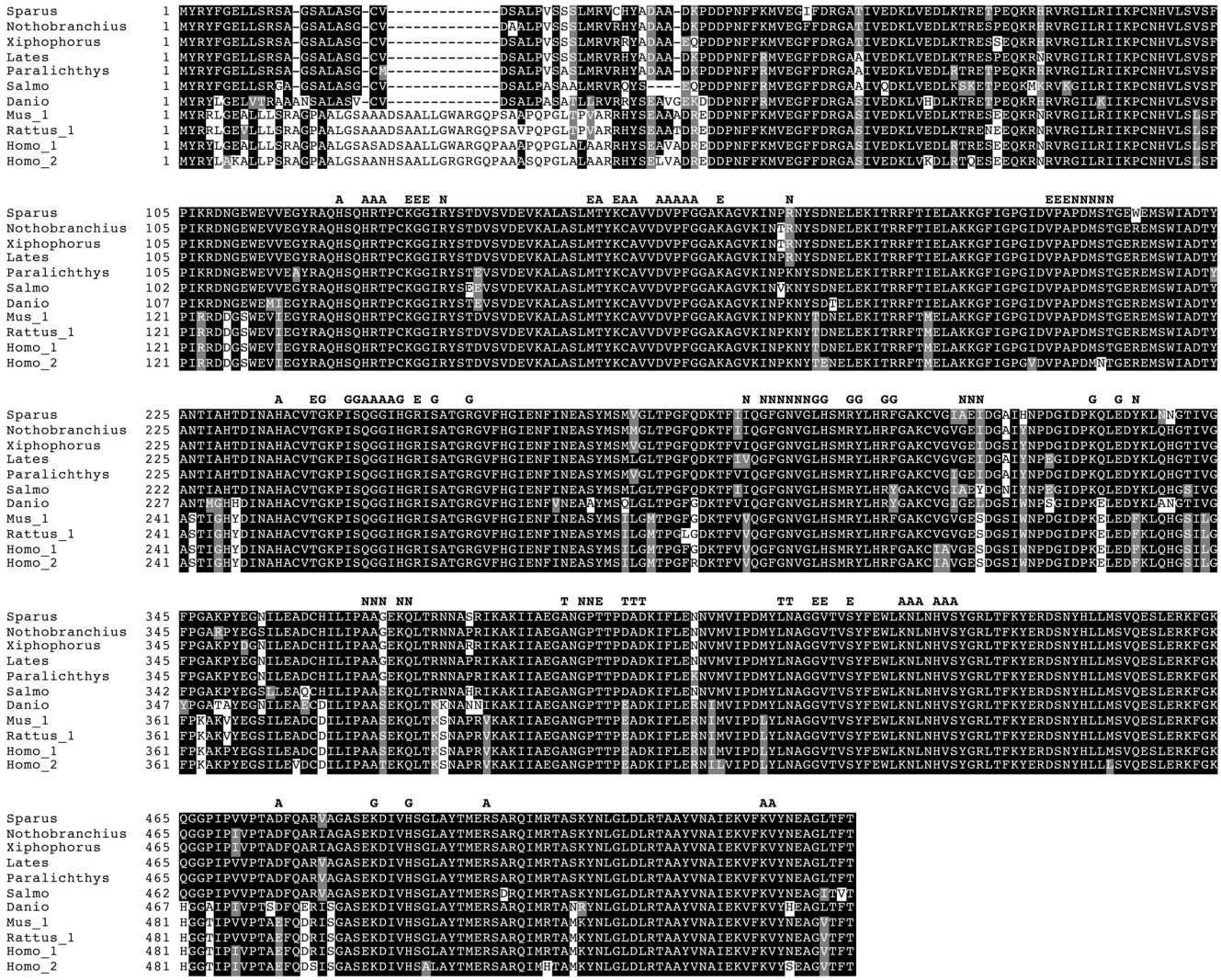
Sparus
Nothobranchius
Xiphophorus
Lates
Paralichthys
Salmo
Danio
Mus_1
Rattus_1
Homo_1
Homo_2

B

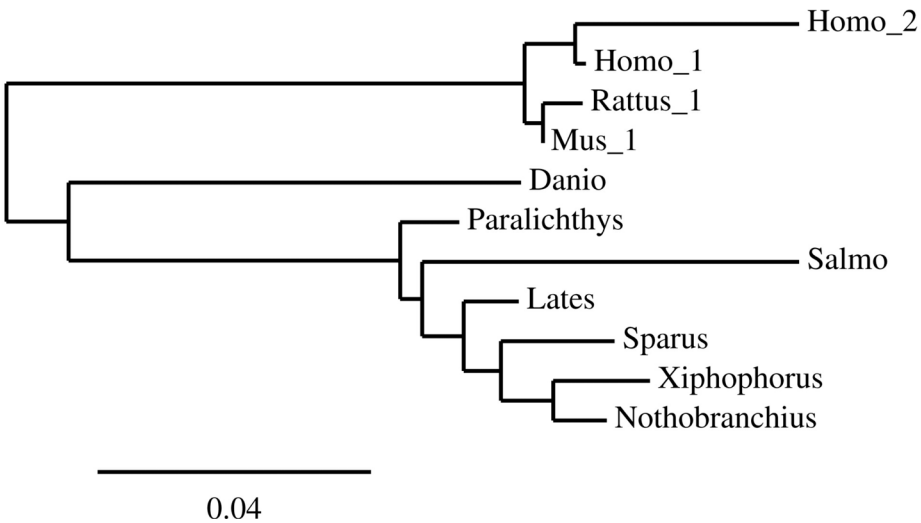
Homo_2
Homo_1
Rattus_1
Mus_1
Danio
Paralichthys
Salmo
Lates
Sparus
Xiphophorus
Nothobranchius
0.04

Figure 2

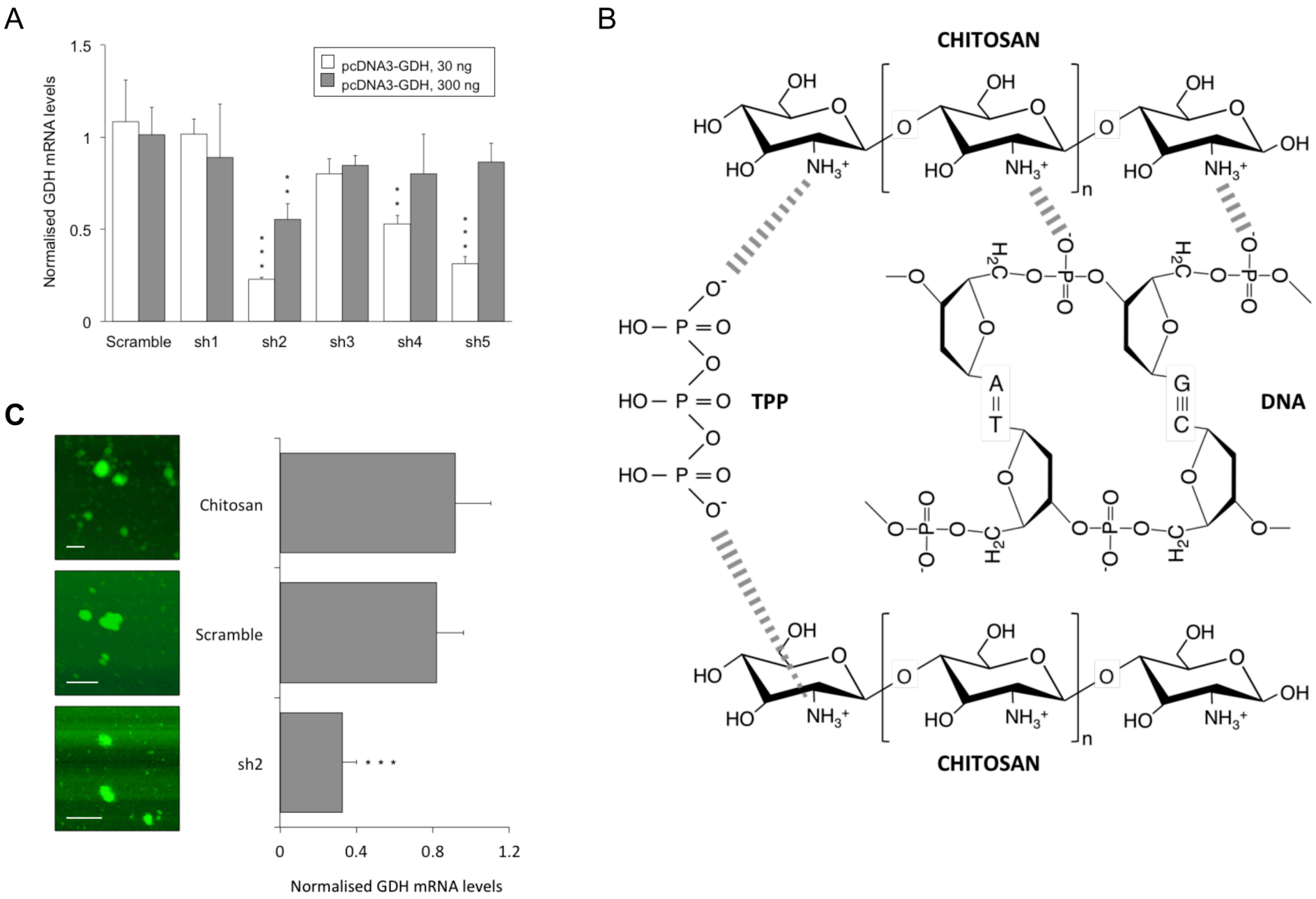
A
1.5
1
0.5
0
Normalised GDH mRNA levels
pcDNA3-GDH, 30 ng
pcDNA3-GDH, 300 ng
Scramble
sh1
sh2
sh3
sh4
sh5
B
CHITOSAN
TPP
DNA
CHITOSAN
C
Chitosan
Scramble
sh2
0
0.4
0.8
1.2
Normalised GDH mRNA levels

Figure 3

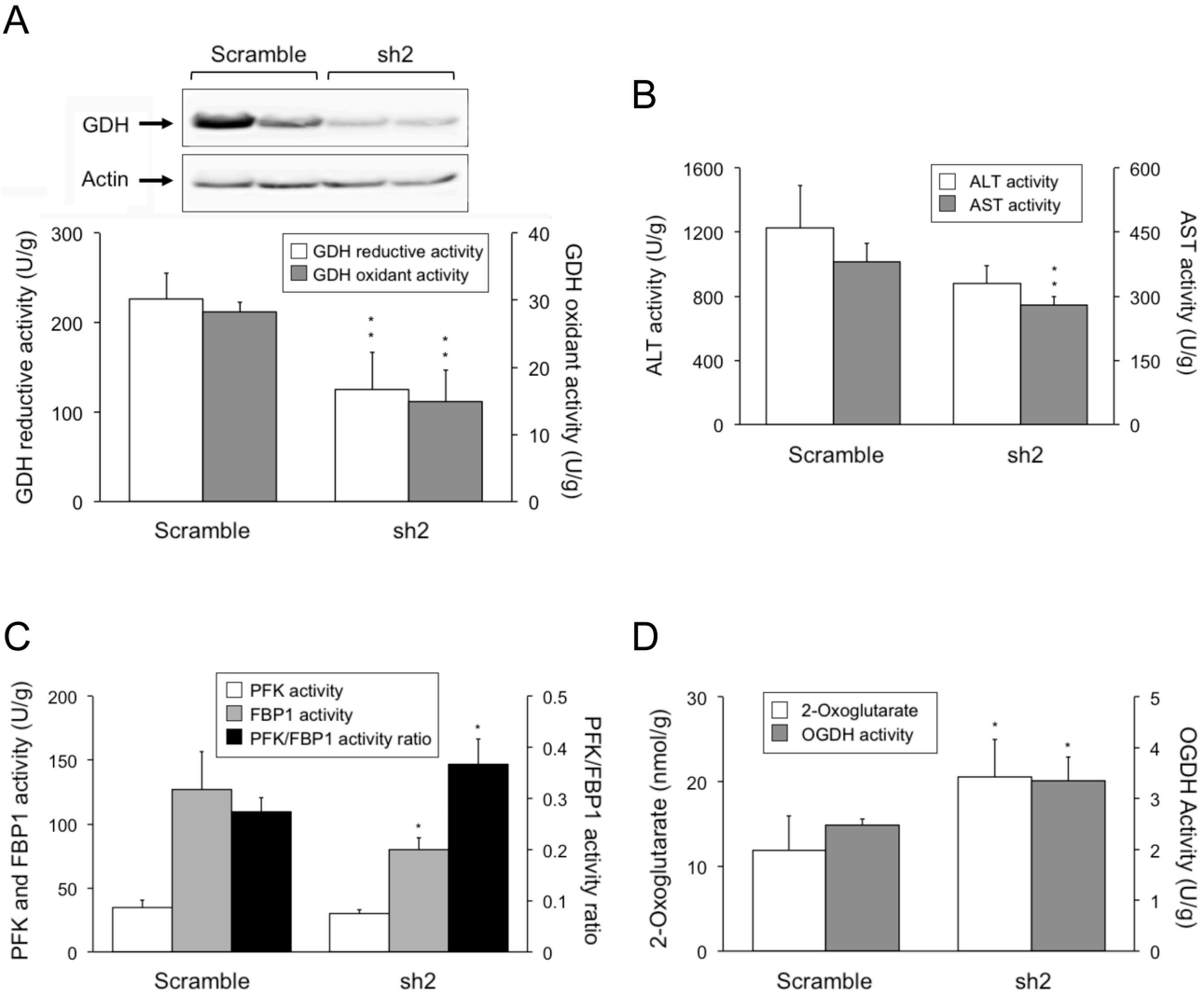
A
Scramble
sh2
GDH
Actin
GDH reductive activity
GDH oxidant activity
GDH reductive activity (U/g)
GDH oxidant activity (U/g)
300
200
100
0
40
30
20
10
0
Scramble
sh2
B
ALT activity
AST activity
ALT activity (U/g)
AST activity (U/g)
1600
1200
800
400
0
600
450
300
150
0
Scramble
sh2
C
PFK activity
FBP1 activity
PFK/FBP1 activity ratio
PFK and FBP1 activity (U/g)
PFK/FBP1 activity ratio
200
150
100
50
0
0.5
0.4
0.3
0.2
0.1
0
Scramble
sh2
D
2-Oxoglutarate
OGDH activity
2-Oxoglutarate (nmol/g)
OGDH Activity (U/g)
30
20
10
0
5
4
3
2
1
0
Scramble
sh2